Electronic Preprint for Journal of Information Processing Vol.27

Regular Paper

# Roadscape-based Route Recommender System Using Coarse-to-fine Route Search

Koji Kawamata[1,a)] Kenta Oku[1,b)]

Received: September 7, 2018, Accepted: January 2, 2019

**Abstract:** We propose Roadscape-based Route Recommender System (R3), which provides diversified roadscape-based routes. Given starting and destination points, R3 provides four types of roadscape-based routes: rural-, mountainous-, waterside-, and urban-prior routes. To reduce the computational cost, we propose a coarse-to-fine route search approach that consists of a roadscape-based clustering method, roadscape cluster graph, coarse-grained route search, and fine-grained route search. We evaluated the performance of R3 using network data for real roads. The experimental results qualitatively show the validity of the generated roadscape clusters by comparing them with Google satellite maps and Google Street View images. The results also show the validity of the roadscape-based route recommendations. Furthermore, the results show that using a coarse-grained route search can significantly reduce the route search time. Finally, we quantitatively evaluate R3 from the perspective of users. The results show that R3 can appropriately recommend roadscape-based routes for given scenarios.

**Keywords:** route recommender system, route search, roadscape

## 1. Introduction

Cars are driven not only for transportation but also for pleasure. Some people want to drive along the seaside or on rural roads while enjoying their favorite landscape. We call such roadside landscapes "roadscapes." In such situations, it is not always the best solution to provide the shortest or fastest route. An alternative solution is to provide routes with favored roadscapes even if they involve a detour.

Given starting and destination points, a route recommender system provides routes from the starting point to the destination point. The majority of traditional route recommender systems provide the shortest routes [15], [28], fastest routes [16], [19], [32], [37], [38], or popular routes [8], [22], [31], [33]. As mentioned above, the shortest and fastest routes do not always satisfy the user's demands. Systems that recommend popular routes provide routes that many people are interested in. Wei et al. [31] extracted popular routes by mining the road links that many people are interested in from their trajectories. Such route recommender systems consider the attractiveness of routes on the basis of the wisdom of crowds without considering the content features of routes. Several studies have proposed scenic route recommender systems [1], [5], [23], [29], [40]. These studies use the subjective scores of the scenic beauty submitted by people and do not focus on the detailed roadscape features of road links.

In this paper, we focus on the roadscape as a route feature and propose Roadscape-based Route Recommender System (R3), which provides diversified routes on the basis of roadscapes. Given starting and destination points, R3 provides four types of roadscape-based routes: rural-, mountainous-, waterside-, and urban-prior routes. For example, a user who likes waterside views can select waterside-prior routes from the four types of routes provided. To develop such a route recommender system, we have proposed a method for estimating the roadscapes of given road links [25], [26]. In particular, we defined rural, mountainous, waterside, and urban elements as roadscape elements, which are basic elements that compose a roadscape, through preliminary experiments. We defined a roadscape vector, each of whose elements corresponds to a roadscape element, and proposed a method for estimating such roadscape vectors for given road links. Although a detailed discussion is beyond the scope of this paper, we instead provide road network data with roadscape vectors on the Web [*1]. We presuppose that R3 is to be used on road network data with roadscape vectors.

Traditional route searching algorithms such as the Dijkstra algorithm [14] are given the costs of road links and find a route that minimizes the sum of their costs. The simplest approach is to apply the traditional method and reduce the costs of the road links having the targeted roadscape elements. However, there is a high computational cost in applying such a method to a very large road network.

To reduce the computational cost, we propose a coarse-to-fine route search approach. We focus on the concept that similar roadscapes do not exist as fragments but in clusters. For example, **Fig. 1** shows that there are some areas composed of similar roadscape elements, such as area A, which is a rural area, and area B, which is a mountainous area. On the basis of this characteristic, we expect that we can reduce the computational cost by clustering

[1] Ryukoku University, Otsu, Shiga 520–2194, Japan
[a)] t18m057@mail.ryukoku.ac.jp
[b)] okukenta@rins.ryukoku.ac.jp

[*1] https://zenodo.org/record/1405255#.W4Yyb-j7T-g

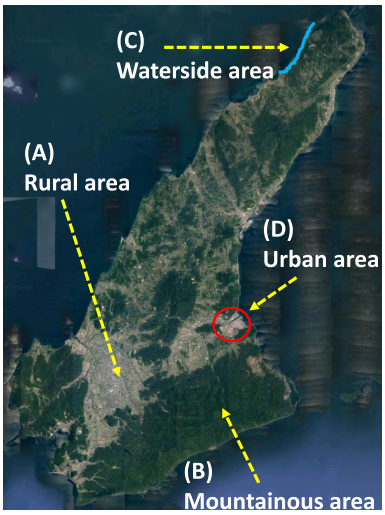


**Fig. 1** Satellite image of Awaji Island, Japan. Area A is a rural area, B is a mountainous area, C is a waterside area, and D is an urban area. This satellite image was captured from Google Maps [*2].

similar roadscape areas in advance.

In this approach, we first extract areas—roadscape clusters—composed of similar roadscape elements by using a roadscape-based clustering method. Second, we create a roadscape cluster graph whose nodes correspond to the roadscape clusters and whose links correspond to the links between roadscape clusters. In the route searching process, given the roadscape cluster graph and starting and destination points, we roughly find four types of roadscape-based routes, which are the roadscape cluster sets passed through, one for each roadscape element; we call this the coarse-grained route search. Then, we find specific routes that connect the roadscape clusters in each type of route; we call this the fine-grained route search.

The contributions of this paper are as follows:

- We propose R3 , which provides diversified roadscape-based routes, namely, rural-, mountainous-, waterside-, and urban-prior routes.
- To reduce the computational cost, we propose a coarse-to-fine route search approach that consists of a roadscape-based clustering method, roadscape cluster graph, coarse-grained route search, and fine-grained route search.
- We evaluate the performance of R3 using network data for real roads. The results show the validity of the generated roadscape clusters and roadscape-based route recommendations. In particular, the results show that using a coarse-grained route search can significantly reduce the route search time.
- We quantitatively evaluate R3 from the perspective of users. The results show that R3 can appropriately recommend roadscape-based routes for given scenarios.

## 2. Related Work

### 2.1 Shortest Routes

There are several well-known algorithms for finding the shortest routes, such as Dijkstra's algorithm [14] and the A* algorithm [13]. Given the starting and destination points, these algorithms find routes that minimize the total cost based on the costs given for the links in the road network.

Many improvements have been proposed for such shortest-route searches. Goldberg et al. [15] improved the route search speed by extending the A* algorithm. Vieria et al. [30] and Potamias et al. [28] proposed a scalable method for large networks.

### 2.2 Fastest Routes

A fastest-route search method finds routes that minimize the time cost based on the travel times given to road links. Kanoulas et al. [19] extracted speed patterns that depend on the time period such as rush hour. They found the fastest routes using a route search algorithm that extends the A* algorithm on the road network with speed patterns. Gonzalez et al. [16] provided a fastest-route search method based on speed patterns mined from large sets of traffic data. Wei et al. [32], given the query time and road links, inferred the mean speed on the road links. They estimated the speed based on speed patterns in GPS data that are spatially and temporally close to the given query time and road links. Yuan et al. [37], [38], given starting and destination points, searched for the fastest routes based on a taxi's GPS trajectory data.

From the perspective of driving pleasure, we consider that it is not always the shortest or fastest routes that are the most pleasant routes for drivers. We hold that it is sometimes useful to recommend routes that go through favored roadscapes even if they make a detour without regard to whether they are the shortest or fastest routes.

### 2.3 Popular Routes

There are many methods for searching for popular routes that may not be the shortest or fastest routes. Chen et al. [8], given starting and destination points, searched for the most popular routes (MPRs) connecting these two points. Here, the MPR is the route with the largest amount of GPS trajectory data and does not necessarily coincide with the shortest or fastest routes. Luo et al. [22] also searched for the MPR using GPS data. They extracted more useful trajectories by referring to a subset of GPS data related to the query time and not all GPS data.

Although the MPR method selects one optimal route, top-$k$ route searching methods output the $k$ routes with the highest route scores. Wei et al. [31] extracted frequently traveled regions from a given set of trajectories and calculated the attractiveness score of each region. They searched for the top $k$ trajectories on the basis of the score. Chen et al. [9] searched for the top $k$ trajectories connecting user-provided locations.

There are also many methods for searching for routes connecting points of interest (POIs), which are extracted from GPS data or geotagged photos. Choudhury et al. [11] extracted the routes connecting POIs in association with POIs and geotagged photos. Yoon et al. [35], [36] extracted stay points from GPS data and extracted the travel sequences between these points. Arase et al. [3] extracted frequent trip patterns, i.e., typical sequences of visited spots, from geotagged photos. Kurashima et al. [20] recommended travel routes connecting key landmarks from geotagged photos posted on Flickr. Lu et al. [21] proposed an auto-

[*2] https://www.google.co.jp/maps/

matic travel route planning method based on geotagged photos. The travel route is automatically planned for the given location to be visited, user preferences, travel duration, visit time, and destination type. Yin et al. [34] extracted diversified trajectory patterns from geotagged photos on Flickr. These studies focus on POIs such as spots and landmarks and extract the routes between POIs, but they do not use the scores of the routes themselves.

Although the above studies focus on finding popular routes using collective intelligence, we focus on the roadscape features of the routes.

### 2.4 Personalized Routes

Some studies propose route searching methods that recommend personalized routes based on users' attributes and preferences. MyRoute [27] generates personalized routes based on routes and landmarks familiar to the user. In MyRoute, users need to specify the landmarks themselves, whereas Going My Way [12] automatically identifies landmarks from users' personal GPS log data. Cheng et al. [10] and Chen et al. [7] proposed a personalized recommendation framework including route planning based on the profiles of users who are contributors of geotagged photos. Chang et al. [6] proposed a personalized route planning framework. Their method extracts familiar road links from a driver's historical trajectory dataset. Then, given starting and destination points, it generates the top $k$ familiar routes. Herzog et al. [17] proposed a mobile personalized route recommender system, RouteMe. Given starting and destination points, RouteMe determines route recommendations by combining collaborative filtering and knowledge-based recommendations.

In R3, users can choose their favorite routes from recommended routes that include four types of diversified roadscape-based routes in route planning. By offering this choice, our system can recommend routes that reflect users' roadscape preferences.

### 2.5 Scenic Routes

#### 2.5.1 Scenic Routes using Subjective Scores

The following studies [1], [5], [23], [29], [40] use subjective scores of the scenic beauty submitted by people and do not focus on the detailed roadscape features of the road links. On the other hand, we focus on objective roadscape features, i.e., rural, mountainous, waterside, and urban elements. We represent road links by roadscape vectors and propose R3, which is based on road network data with roadscape vectors.

Alivand et al. [1] proposed a method for extracting scenic routes from geotagged photos and Volunteered Geographic Information (VGI) routes. They associate geotagged photos, which are uploaded to Panoramio and Flickr, with a road network and extract routes where photos are densely distributed as scenic routes. VGI routes are traveled routes that are uploaded to websites such as RouteYou [*3], EveryTrail [*4], and MyScenicDrive [*5]. They extract scenic routes from these VGI routes. Their approach is based on the assumption of "travelers typically share photos or their trip trajectory with the Web community when they consider a place or trip scenic [18]."

Zheng et al. [40] define a scenic roadway as "a thoroughfare that passes by a series of landscapes and sights and affords vistas of notable aesthetic, geological, historical, cultural, and touristic qualities along its roadside." They propose an attention-based approach to discover scenic roadways from geotagged photos. They explain that "if a large number of photos are densely distributed along a roadway, this roadway is a scenic one." They calculate the visibility on the basis of the distribution of photos related to the roadway and the popularity on the basis of the number of photos. Then, they calculate the sightseeing score by combining the visibility and popularity. They update a road link's cost by decreasing the sightseeing scores from its length. Given the updated road network, existing shortest path algorithms such as Dijkstra's algorithm [14] and the Bellman–Ford algorithm [4] are used.

Byon et al. [5] define a scenic route as "a route with visually pleasing sights." They built a scenic view layer (SVL) that consists of a visibility layer (VL) and zonal scenic worth raster layer (ZSWRL). They divided Tronto into thirteen zones, and each zone was rated by travel agents from the viewpoint of whether the zone is scenic in a preliminary survey. The ZSWRL was built on the basis of the results of the survey. The VL as built on the basis of the visibility of each zone from each road link. On the basis of the SVL, the costs on a road network are updated. Given the updated road network, existing shortest path algorithms such as Dijkstra's algorithm [14] are used.

Quercia et al. [29] recommend routes that are not only short but also emotionally pleasant. They assign the labels "beautiful," "quiet," and "happy" to locations by crowdsourcing. They then calculate the scores for the locations on the basis of their labels. Finally, they recommend the shortest, most beautiful, most quiet, and happiest routes on the basis of the respective scores.

Manzaki et al. [23] proposed a Country Road Finder. They focus on the scenic beauty from driver's viewpoint. Their system generates three routes from a location—a farm—that a user selected to the nearest three lodges. On the basis of Google Street View images along each route, the scenic beauty scores of each route are predicted using deep learning. In training phase, the scenic beauty of each Street View image is manually given.

#### 2.5.2 Scenic Routes using Objective Scores

Niaraki et al. [24] focused on roadscape factors as road attributes. They define road attributes by ontology. Because their ontology includes roadscape attributes, their system can provide roadscape-based routes by using such attributes. However, although the ontology framework is described in detail, they do not mention how to construct the ontology.

Alivand et al. [2] analyzed the influence of the existence of water bodies, mountains, parks, and urban areas in addition to geotagged photos and VGI routes [1] on a route choice model. However, their study focuses on analyzing people's route choice model, and their method for extracting scenic routes includes manual processes. On the other hand, we focus on a route recommender system that automates whole processes from vectorizing the roadscape features of road links to recommending roadscape-based routes.

[*3] http://www.routeyou.com/
[*4] http://www.everytrail.com
[*5] http://www.myscenicdrives.com/

Zhang et al. [39] proposed scenic sights as "landscapes that can be enjoyed as a distant view," such as Mt. Fuji, the Eiffel Tower, and the Gate of Heavenly Peace. They collect scenic sights from the Web. Then they calculate the visibility of each road node toward the sights using the notion of a Z-Buffer on a virtual 3D space built on the basis of a digital elevation map (DEM). Recommended routes between starting and destination points are ranked in descending order of the visibility scores. Although their method uses scenic sights, the landscape features of the road links are not used.

Hochmair et al. [18] define a scenic route as "a route that maximizes the exposure to parks and water bodies and minimizes detours." Their basic idea is to reduce the costs of the road links that are close to attractive locations. They take parks and water bodies as attractive locations. Using the notion of buffering, they reduce the costs of the road links within a certain buffer distance around attractive locations. Given the updated road network, existing shortest path algorithms such as Dijkstra's algorithm [14] are used. Although their method uses a single cost by aggregating multiple elements such as parks and water bodies, our method uses multiple costs as a cost vector, which enables the generation of diversified roadscape-based routes, namely, rural-, mountainous-, waterside-, and urban prior routes.

## 3. Preliminaries

**Definition 1: Road network.** A road network is a directed weighted graph $G = (V, E)$, where $V$ is a set of road nodes and $E \subseteq V \times V$ is a set of road links. A road node $v_i \in V$ represents an intersection or an endpoint of a road. A road link $e_k = (v_i, v_j) \in E$ is a directed link from the starting node $v_i$ to the ending node $v_j$. A road link $e_k$ is assigned a cost $w_k$ according to the length of the link.

**Definition 2: Roadscape element.** Roadscape elements are basic elements that compose a roadscape. We define four roadscape elements: rural, mountainous, waterside, and urban elements. These elements were selected by preliminary experimentation [*6].

**Definition 3: Roadscape vector.** A roadscape vector is defined as a four-dimensional probability vector each of whose elements corresponds to one of the respective roadscape elements. We define a roadscape vector of a road link $e_i$ as $\boldsymbol{s}(e_i) = (s_i^r, s_i^m, s_i^w, s_i^u)$. Each element of the vector denotes the probability of how strongly $e_i$ includes the corresponding roadscape element. Therefore, the sum of the values over all elements is 1.

**Definition 4: Roadscape cluster.** A roadscape cluster $C_j \in C$ is represented by a set of road links having similar roadscape vectors. A roadscape vector $\boldsymbol{s}(C_j)$ of roadscape cluster $C_j$ is represented by the mean vector of the roadscape vectors of the road links included in cluster $C_j$. Therefore, we define $\boldsymbol{s}(C_j)$ as follows:

$$\boldsymbol{s}(C_j) = \frac{1}{|C_j|} \sum_{i \in C_j} \boldsymbol{s}(e_i). \tag{1}$$

Here, $|C_j|$ denotes the number of road links included in the roadscape cluster $C_j$.

**Definition 5: Roadscape cluster graph.** A roadscape cluster graph is a directed weighted graph $\mathcal{G} = (\mathcal{V}, \mathcal{E})$, where $\mathcal{V}$ is a set of roadscape clusters $C_i$ and $\mathcal{E} \subseteq \mathcal{V} \times \mathcal{V}$ is a set of links between roadscape clusters. A link $l_k = (C_i, C_j) \in \mathcal{E}$ is a directed link from the starting node $C_i$ to the ending node $C_j$. The road link $l_k$ is assigned a cost vector $\boldsymbol{\omega_k} = (\omega_k^r, \omega_k^m, \omega_k^w, \omega_k^u)$ based on the roadscape vector $\boldsymbol{C}_j$ of ending roadscape cluster $C_j$. Each element of $\boldsymbol{\omega_k}$ denotes a cost for the corresponding roadscape; these are used for roadscape-based route searching. For example, $\omega_k^r$ is the cost referenced when searching for rural-prior routes.

**Definition 6: Intracluster similarity of a roadscape vector.** The intracluster similarity is the mean similarity between all pairs of road links included in the cluster. We denote the intracluster similarity of roadscape cluster $C_j$ as intra_sim($C_j$). The value of intra_sim($C_j$) is calculated as follows:

$$\text{intra\_sim}(C_j) = \frac{1}{n|C_j|} \sum_{i \in C_j} \sum_{k \in C_j} \cos(\boldsymbol{s}(e_i), \boldsymbol{s}(e_k)). \tag{2}$$

Here, $e_i$ and $e_k$ are road links included in cluster $C_j$, and $n$ denotes the total number of links in the road network. The value of $\cos(\boldsymbol{s}(e_i), \boldsymbol{s}(e_k))$ is calculated as follows:

$$\cos(\boldsymbol{s}(e_i), \boldsymbol{s}(e_k)) = \frac{\boldsymbol{s}(e_i) \cdot \boldsymbol{s}(e_k)}{|\boldsymbol{s}(e_i)||\boldsymbol{s}(e_k)|}. \tag{3}$$

## 4. Roadscape-based Route Recommender System

### 4.1 System Overview

R3 provides four types of roadscape-based routes: rural-, mountainous-, waterside-, and urban-prior routes. **Figure 2**

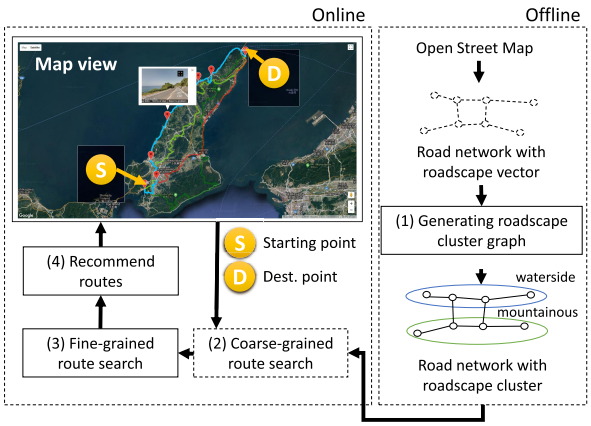


**Fig. 2** An R3 interface and its system configuration. (1) Generate a roadscape cluster graph based on the road network with roadscape vectors. (2) Roughly find four types of roadscape-based routes in the roadscape cluster graph based on the starting and destination points that are input. (3) Find a detailed route that connects roadscape clusters of each type. (4) Recommend four types of routes in different colors on the map view. The map view is shown by using Google Maps API [*7].

[*6] The preliminary experimentation to select the roadscape elements was done via crowdsourcing. These four elements are specific to Japanese road network data. The details are beyond the scope of this paper.

[*7] https://cloud.google.com/maps-platform/maps/?apis=maps

shows an R3 interface and its system configuration. The interface has a map view. When a user inputs the starting and destination points on the map, the four types of roadscape-based routes are provided in different colors.

It is assumed that R3 will be used with a road network with roadscape vectors. In the evaluation (see Section 5), we used a road network with roadscape vectors, which is available on the web [*1]. Note that an explanation of how such road network data can be generated is beyond the scope of this paper. The steps of R3 are as follows (the step numbers correspond to the numbers in Fig. 2):

(1) Generate a roadscape cluster graph based on the road network with roadscape vectors.
(2) Roughly find four types of roadscape-based routes in the roadscape cluster graph based on the starting and destination points that are input (coarse-grained route search).
(3) Find a detailed route that connects roadscape clusters of each type (fine-grained route search).
(4) Recommend four types of routes in different colors on the map view.

Here, step (1) can be performed offline because this process does not depend on the inputs. In the next sections, we describe steps (1)–(3) in detail.

### 4.2 Generating a Roadscape Cluster Graph

#### 4.2.1 Roadscape-based Clustering

Given a road network, we form roadscape clusters on the basis of proximities of pairs of road links and the similarities between their roadscape vectors. Adjacent road links belong to the same cluster if their similarity is greater than or equal to a given threshold value. **Figure 3** shows the result of applying roadscape-based clustering to the road network of Awaji Island, Japan. As we can see in Fig. 1, area A corresponds to a rural area, and area B corresponds to a mountainous area.

Algorithm 1 shows the pseudocode for roadscape-based clustering. We explain the clustering process performed by Algorithm 1 as follows:

First, let $k = 1$ be the initial value (line 1). This $k$ corresponds to the index $k$ of cluster $C_k$ that is the current focus. Each road link $e_i \in E$ will be added to the relevant cluster $C_k$ (lines 2–8). However, if $e_i$ has already been a member of any cluster, skip the following processes (lines 3–5). Roadscape-based clustering is executed by calling the function `roadscapeCluster`($\boldsymbol{s}(e_i), e_i, k$) (line 6). Here, $\boldsymbol{s}(e_i)$ is a roadscape vector of link $e_i$. We consider this roadscape vector $\boldsymbol{s}(e_i)$ as a reference vector for calculating the similarity of roadscape vectors in clustering for the current cluster $C_k$.

The function `roadscapeCluster`() has three arguments, a roadscape vector $\boldsymbol{s}$, a target road link $e$, and the index of cluster $C_k$ (lines 9–20). First, add the target road link $e$ to cluster $C_k$ (line 10). Call the function getAdjLinks($e$) that obtains the links adjacent to link $e$ and add the obtained links to `adjLinkList` (line 11). Here, if two links are connected to a common node, the links are considered adjacent. **Figure 4** shows an example of a road network. In this case, for example, the links adjacent to $e_3$ are $\{e_1, e_2, e_4, e_5, e_6\}$.

Consider each link $e_j$ in `adjLinkList` (lines 12–19). However, if $e_j$ has already been a member of any cluster, skip the following processes (lines 13–15). Calculate the cosine sim-

**Algorithm 1** Roadscape-based clustering.

```
1: k ⇐ 1
2: for each link e_i ∈ E
3:     if e_i is a member of any cluster then
4:         continue next link
5:     end if
6:     roadscapeCluster(s(e_i), e_i, k)
7:     k ⇐ k + 1
8: end for
9: function ROADSCAPECLUSTER(s, e, k)
10:    add e to cluster C_k
11:    adjLinkList ⇐ getAdjLinks(e): Get links adjacent to e.
12:    for each link e_j in adjLinkList
13:        if e_j is a member of any cluster then
14:            continue next link
15:        end if
16:        if cos(s, s(e_j)) >= α then
17:            roadscapeCluster(s, e_j, k)
18:        end if
19:    end for
20: end function
```

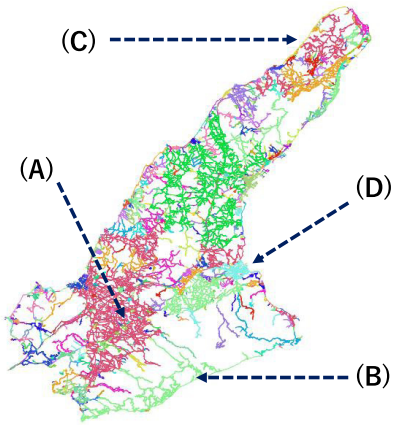


**Fig. 3** Result of applying roadscape-based clustering to the road network of Awaji Island, Japan. Each color corresponds to a given cluster. Labels A–D correspond to the same labels in Fig. 1.

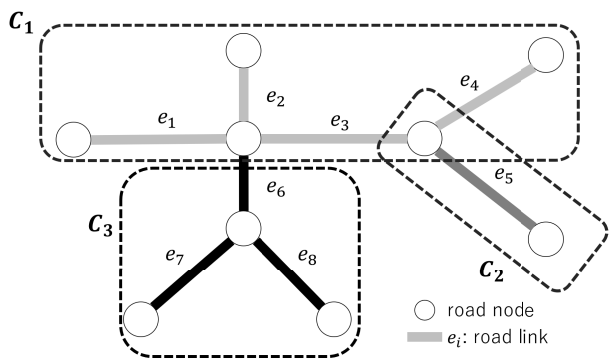


**Fig. 4** A toy example of roadscape-based clustering on a small road network. $e_i$ denotes the $i$th road link. The color intensity of a link denotes the roadscape vector. If the color intensity of two links are equivalent, these links have similar roadscapes. $C_k$ denotes the $k$th cluster.

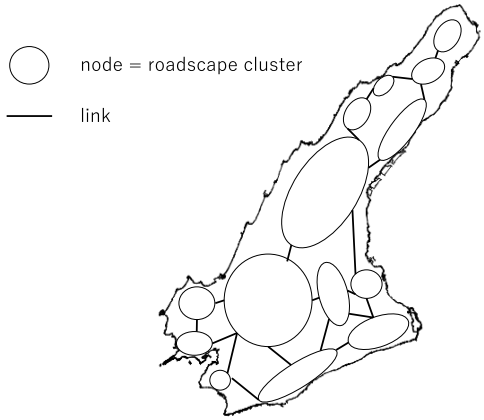


**Fig. 5** Example of a roadscape cluster graph created for Awaji Island's road network. A node in the roadscape cluster graph corresponds to a roadscape cluster, and a link corresponds to the adjacency relationship between clusters.

ilarity $\cos(\boldsymbol{s}, \boldsymbol{s}(e_j))$ (Eq. (3)) between roadscape vectors $\boldsymbol{s}$ and $\boldsymbol{s}(e_j)$. If $\cos(\boldsymbol{s}, \boldsymbol{s}(e_j))$ is greater than or equal to the threshold $\alpha$, `roadscapeCluster`$(\boldsymbol{s}, \boldsymbol{s}(e_j), k)$ is recursively called (lines 16–18).

After finishing this clustering process for the current cluster $C_k$, increment $k$ by one and repeat the same process for the remaining road links (line 7). The above process is repeated until all of the links in the road network have been added to any cluster. Finally, roadscape vector $\boldsymbol{s}(C_k)$ of cluster $C_k$ is calculated by Eq. (1).

Figure 4 shows a toy example of roadscape-based clustering on a small road network. Here, $e_i$ denotes the $i$th road link. The color intensity of a link denotes the roadscape vector. If the color intensity of two links are equivalent, these links have similar roadscapes. $C_k$ denotes the $k$th cluster. In this case, links $\{e_1, e_2, e_3, e_4\}$ are added to cluster $C_1$, link $\{e_5\}$ is added to cluster $C_2$, and links $\{e_6, e_7, e_8\}$ are added to cluster $C_3$.

#### 4.2.2 Generating a Roadscape Cluster Graph

After extracting the roadscape clusters, we create the adjacency matrix for all roadscape clusters. The adjacency matrix for the roadscape clusters is represented as the $|C| \times |C|$ matrix $\mathcal{A} = [a_{ij}]_{|C|\times|C|}$. If $a_{ij} = 1$, clusters $C_i$ and $C_j$ have at least one common node; otherwise, they do not have a common node.

We then create the roadscape cluster graph on the basis of the adjacency matrix. **Figure 5** gives an example of the roadscape cluster graph created for Awaji Island's road network. Here, a node in the roadscape cluster graph corresponds to a roadscape cluster, and a link corresponds to the adjacency relationship between clusters.

#### 4.2.3 Assigning Costs to a Roadscape Cluster Graph

In order to execute the coarse-grained route search described in the next section, we assign costs to the links of the roadscape cluster graph in advance. A link cost is calculated on the basis of the roadscape vector of the roadscape cluster corresponding to the link's destination. If the targeted roadscape element of the next roadscape cluster destination is emphasized, let its link cost be lower; on the other hand, if it is not emphasized, let its link cost be higher. For example, for the case in which a rural element is targeted, if the rural element of the next roadscape cluster destination is emphasized, let its link cost be lower; otherwise, let its link cost be higher. By assigning costs in such a way, the route to the roadscape cluster where the rural element is emphasized is more likely to be chosen in the route search.

A cost vector $\boldsymbol{\omega}_k$ of link $l_k = (C_i, C_j)$ is calculated as follows:

$$\boldsymbol{\omega}_k = d_k(1 - \boldsymbol{s}(C_j)^2). \tag{4}$$

Here, $d_k$ is the length of link $l_k$.

### 4.3 Coarse-grained Route Search

As the first search, we execute the coarse-grained route search method. This method roughly finds four types of roadscape-based routes in the roadscape cluster graph. The process is as follows:

(1) Given starting and destination points, obtain the roadscape clusters and the starting and destination clusters, which include the starting and destination points, respectively.
(2) For the targeted roadscape element, find a route that minimizes the sum of the link costs related to the targeted elements using existing shortest path algorithms such as Dijkstra's algorithm [14] on the roadscape cluster graph.
(3) Repeat step (2) for each roadscape element.

Thus, we obtain four types of coarse-grained routes as the roadscape cluster sets that are passed through for each roadscape element.

### 4.4 Fine-grained Route Search

As the second search, we execute the fine-grained route search method for each coarse-grained route. This method finds detailed routes that connect roadscape clusters. The process for each targeted element is as follows:

(1) Find the common road nodes of each adjacent cluster in the roadscape cluster sets captured by the coarse-grained route search.
(2) Find the shortest route from the starting point to the first common road node that is adjacent to the next cluster.
(3) Until there are common road nodes, find the shortest route from the common road node to the next common node.
(4) Find the shortest route from the last common node to the destination point.
(5) Generate a route that connects all of the routes obtained.

Here, we again use existing shortest path algorithms such as Dijkstra's algorithm to find the shortest routes. Finally, we obtain four types of fine-grained routes: rural, mountainous, waterside, and urban routes.

## 5. Results

In this section, we evaluate the performance of R3 using network data for real roads in Awaji Island, Japan. The road network data are derived from OpenStreetMap [*8], and they include 102,506 road nodes and 212,050 road links for the area of Awaji Island. For this area, roadscape vectors for all road links are available on the web [*1]. We evaluate the validity of the generated roadscape clusters and the validity of the roadscape-based route recommendations, and we compare the route search times of R3 with and without the use of the coarse-grained route search.

[*8] https://www.openstreetmap.org/

**Table 1** Results of roadscape-based clustering according to the value of $\alpha$. For each value of $\alpha$, this table lists the number of generated clusters, the mean number of links included in each cluster, and the mean value of the intracluster similarities of the roadscape vectors.

| $\alpha$ | # clusters | mean # links included in cluster | intra-cluster similarity |
|---|---|---|---|
| 0.95 | 4896 | 43.3 | **0.989** |
| 0.90 | 2912 | 72.8 | 0.980 |
| 0.85 | 2111 | 100.5 | 0.972 |
| 0.80 | 1538 | 137.9 | 0.962 |
| 0.75 | 1158 | 183.1 | 0.939 |
| 0.70 | 1094 | 193.8 | 0.948 |
| 0.65 | 718 | 295.3 | 0.833 |

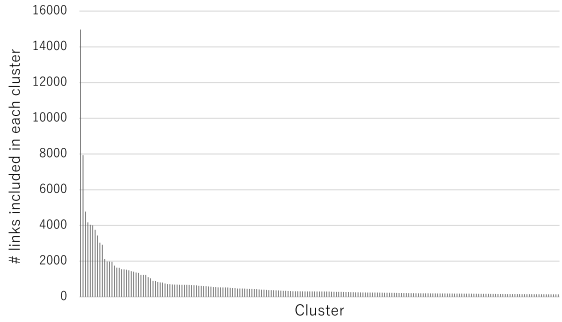


**Fig. 6** Distribution of the number of links belonging to the clusters when $\alpha = 0.95$. The horizontal axis denotes the clusters in descending order of the number of links, and the vertical axis denotes the number of links included in the cluster. Only the top 100 clusters are listed.

### 5.1 Study of the Parameter $\alpha$

We determine the threshold $\alpha$ for the similarity between roadscape vectors, which is needed for the roadscape-based clustering described in Section 4.2.1. Roadscape-based clustering was performed while varying $\alpha$ among the values $\alpha = \{0.95, 0.90, 0.85, 0.80, 0.75, 0.70, 0.65\}$ for Awaji Island's road network.

**Table 1** summarizes the results of clustering for each value of $\alpha$. The table lists the number of clusters generated for each value of $\alpha$, the mean number of links included in each cluster, and the mean value of the intracluster similarities of the roadscape vectors. More clusters were generated when the $\alpha$ value was higher. In addition, when $\alpha = 0.95$, the intracluster similarity between roadscape vectors was the highest. We can see that with $\alpha = 0.95$, each cluster is formed by road links having similar roadscapes; therefore, clusters are well-generated. As a result, in the subsequent evaluation, we employ $\alpha = 0.95$.

We focus on the distribution of the number of links included in the generated roadscape clusters. Table 1 summarizes the mean number of links included in each cluster. In fact, some clusters have a great many links, and others have few links—zero in most clusters. The variance of the number of links in each cluster is large. **Figure 6** shows the distribution of the number of links included in the clusters when $\alpha = 0.95$. The horizontal axis represents the clusters in descending order of the number of links, and the vertical axis represents the number of links included in the cluster. Only the top 100 clusters are shown because the number of clusters is very large. We can see from Fig. 6 that the majority of clusters have very few links.

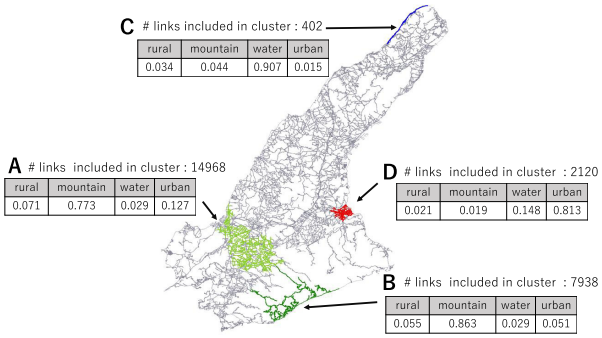


**Fig. 7** Results of roadscape-based clustering on the Awaji Island road network data. The light green area (A) corresponds to a roadscape cluster with a high number of rural elements, the dark green area (B) corresponds to one with a high number of mountainous elements, the blue area (C) corresponds to one with a high number of waterside elements, and the red area (D) corresponds to one with a high number of urban elements. This figure shows the roadscape vector and the number of links for each cluster. Labels A–D correspond to the same labels in Fig. 1.

(a) Area A. (b) Area B.

(c) Area C. (d) Area D.

**Fig. 8** Google Street View images of representative road links in each roadscape cluster. Areas A–D correspond to Areas A–D in Fig. 7. These images were captured from Google Street View.

### 5.2 Validity of the Generated Roadscape Clusters

In this section, we evaluate the validity of the generated roadscape clusters when $\alpha = 0.95$.

**Figure 7** shows the results of roadscape-based clustering on the road network of Awaji Island, showing only the four representative clusters. In Fig. 7, the light green area (A) corresponds to a roadscape cluster with a high number of rural elements, the dark green area (B) corresponds to a cluster with a high number of mountainous elements, the blue area (C) corresponds to a cluster with a high number of waterside elements, and the red area (D) corresponds to a cluster with a high number of urban elements. The figure shows the roadscape vector and the number of links for each cluster. For comparison, Fig. 1 shows a satellite image of Awaji Island. Furthermore, **Fig. 8** shows Google Street View images of representative road links arbitrarily extracted from each cluster.

We discuss the results of roadscape-based clustering in Fig. 7 with reference to Fig. 1 and Fig. 8.

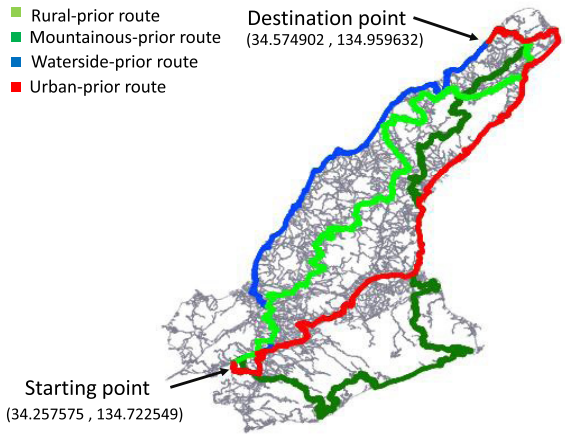


**Fig. 9** Recommended routes when setting the starting point as 34.257575°N, 134.722549°E and the destination point as 34.574902°N, 134.959632°E. The light green line corresponds to a rural-prior route, the dark green line corresponds to a mountainous-prior route, the blue line corresponds to a waterside-prior route, and the red line corresponds to an urban-prior route. The threshold of similarity for roadscape-based clustering was $\alpha = 0.95$.

**(a) Area A.**

Area A corresponds to a roadscape cluster having a high number of rural elements. We can see from Fig. 1 that the rural region is spread throughout area A. We can also see fields in Fig. 8 (a).

**(b) Area B.**

Area B corresponds to a roadscape cluster having a high number of mountainous elements. We can see from Fig. 1 that the mountainous region is spread throughout area B. We can also see tree-covered views in Fig. 8 (b).

**(c) Area C.**

Area C corresponds to a roadscape cluster having a high number of waterside elements. We can see from Fig. 1 that the road links run along the coast. We can also see the coast in Fig. 8 (c).

**(d) Area D.**

Area D corresponds to a roadscape cluster having a high number of urban elements. Area D in Fig. 7 corresponds to a city region. We can also see buildings in Fig. 8 (d).

Because the appropriate results were observed in each area, we can say that the roadscape-based clustering method works well.

### 5.3 Validity of Roadscape-based Route Recommendations

Given starting and destination points, R3 provides roadscape-based routes connecting these two points. The system provides four patterns of routes having high numbers of rural, mountainous, waterside, and urban elements as roadscape-based routes. In this section, we qualitatively and quantitatively evaluate the validity of the routes provided.

First, we qualitatively evaluate the validity of the recommended roadscape-based routes. **Figure 9** shows the recommended routes when the starting point was set as 34.257575°N, 134.722549°E and the destination point as 34.574902°N, 134.959632°E. The light green line corresponds to a rural-prior route, the dark green line corresponds to a mountainous-prior route, the blue line corresponds to a waterside-prior route, and the red line corresponds to an urban-prior route. The threshold of similarity for the roadscape-based clustering was $\alpha = 0.95$.

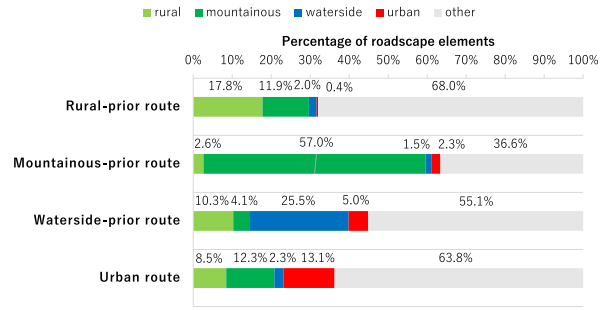


**Fig. 10** Percentages of roadscape elements included in each recommended route. The percentage denotes the proportion of the length of road links having high numbers of roadscape elements when letting the total length of each route be 100%. Road links having a high number of roadscape elements are defined to be those with a roadscape element value of not less than 0.8 in the associated roadscape vector.

We can see from Fig. 9 that various routes were recommended, each one emphasizing a different roadscape element. The rural-prior route passes through the rural area in the inland part of Awaji Island. The mountainous-prior route passes through the mountainous area in the south. The waterside-prior route is a route along the coastline. The urban-prior route is a route passing through Sumoto city, which is the city of Awaji Island.

Furthermore, we quantitatively analyze the tendency for roadscape elements to be included in each recommended route. **Figure 10** shows the percentages of roadscape elements included in each route. The percentage denotes the proportion of the length of road links having high numbers of roadscape elements when letting the total length of each route be 100%. Road links having a high number of roadscape elements are defined to be those with a roadscape element value of not less than 0.8 in the associated roadscape vector. We can see from Fig. 10 that the rural-prior route is occupied by rural elements, the mountainous-prior route by mountainous elements, the waterside-prior route by waterside elements, and the urban-prior route by urban elements.

Thus, we have qualitatively and quantitatively confirmed that R3 can provide routes reflecting each roadscape element.

### 5.4 Comparison of Route Search Times: With vs. Without the Coarse-grained Route Search

R3 introduces a coarse-grained route search as preprocessing to reduce the route search time instead of performing a route search on all road links. In this section, we compare the route search times using the coarse-grained route search with those not using it.

First, we prepare the following five pairs of starting and destination points.

(a) (34.257575, 134.722549) → (34.257575, 134.722549),
(b) (34.317774, 134.676412) → (34.348304, 134.896255),
(c) (34.499798, 134.938260) → (34.293801, 134.788816),
(d) (34.545838, 134.923368) → (34.440009, 134.912038),
(e) (34.208185, 134.814500) → (34.430861, 134.830634).

For each pair, we execute the route search algorithm that emphasizes each roadscape element and measure the route search time. We regard this execution as one trial. We execute this trial 10

times for each pair and calculate the mean of the route search times across trials.

We implemented the route search algorithm using Python 3.6.6 and NetworkX 2.1 and managed the road network data using PostgreSQL 9.5. We conducted experiments on a computer equipped with an Intel Core i5-6200U CPU (2.8 GHz), 8 GB of memory, a 256 GB SSD, and Linux Mint 18.2.

As we described in Section 4.3 and Section 4.4, our algorithm uses an existing shortest path algorithm on an updated road network. Such an approach is employed in most exiting methods for scenic route search [5], [18], [40], as shown in Section 2.5. Therefore, we consider that comparing our algorithm with existing shortest path algorithms is sufficient for a comparison of route search times. We take Dijkstra's algorithm [14] and the A* algorithm [13], which are well-known algorithms, and the Bellman–Ford algorithm [4], which is used in Ref. [40], as baselines.

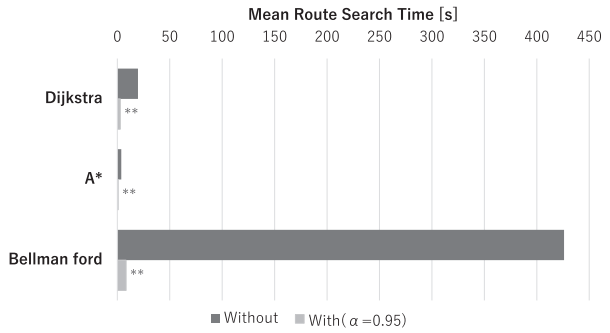


**Fig. 11** Comparison of route search times. This figure shows the mean route search times of methods with and without the coarse-grained route search for each algorithm. For the method with the coarse-grained route search, the figure shows the route search time in the case of $\alpha = 0.95$. ** indicates that a significant difference ($p < 0.01$) could be confirmed when comparing with the method without the coarse-grained route search by a paired $t$-test (one-sided test).

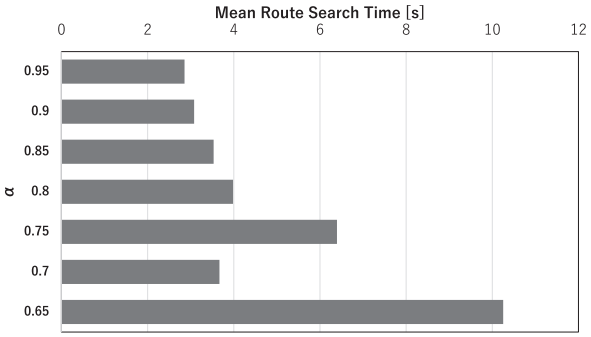


**Fig. 12** Comparison of route search times for each value of $\alpha$. The method with the coarse-grained route search based on Dijkstra's algorithm is used for comparison.

In this experiment, we compare the route search times using coarse-grained route search with those not using it based on these three existing algorithms. **Figure 11** shows the mean route search times for methods with and without the coarse-grained route search for each algorithm. Here, the methods without the coarse-grained route search based on Dijkstra's, A*, and Bellman–ford algorithms are regarded as baselines. For the methods with the coarse-grained route search, the figure shows the route search time in the case of $\alpha = 0.95$. ** indicates that a significant difference ($p < 0.01$) could be confirmed when comparing with the method without the coarse-grained route search by a paired $t$-test (one-sided test). We can see from these results that the route search time can be shortened by using the coarse-grained route search through these three algorithms. Consequently, we can say that the use of the coarse-grained route search can significantly reduce the route search time.

In the case of the method with the coarse-grained route search based on Dijkstra's algorithm, we also compare the route search times for each value of $\alpha$. **Figure 12** shows the route search time for each value of $\alpha$. The figure shows that a higher value of $\alpha$ results in a shorter route search time.

## 6. User Evaluation

We quantitatively evaluated R3 from a user perspective. Given the same starting and destination points, we tested five routes: the shortest (baseline) route and rural-, mountainous-, waterside-, and urban-prior routes. For the process of this user evaluation, refer to the user assessment given in Ref. [29].

### 6.1 Experimental Setup

Our participants saw the five different routes between the same starting and destination points on a web page, as shown in **Fig. 13**. They did not know which route was which. The routes provided were shown as routes highlighted on a map and satellite images, and Street View images were shown for five waypoints (see **Fig. 14**). For these, we selected waypoints that were 1/6, 2/6, 3/6, 4/6, and 5/6 of the way along the route.

We provided the following four scenarios to the participants: (s1) *I want to enjoy driving through rural landscapes*, (s2) *I want to enjoy driving through mountainous landscapes*, (s3) *I want to enjoy driving through waterside landscapes*, and (s4) *I want to enjoy driving through urban landscapes*. The participants imagined each scenario and evaluated the suitableness of the five routes for the given scenarios. To measure the suitableness, we used the Likert scale (strongly suitable, suitable, neither suitable

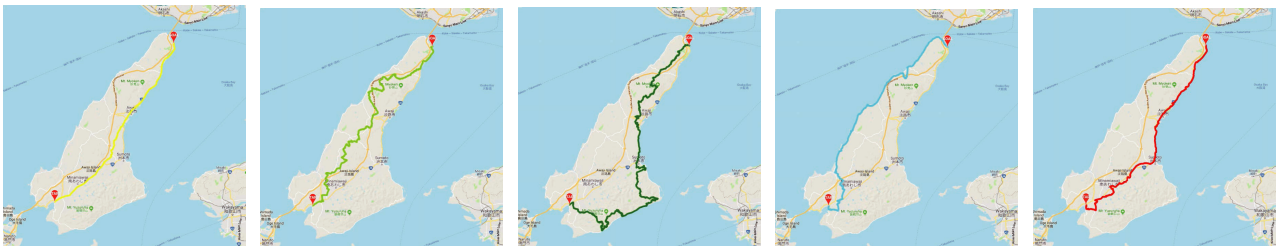

(a) Shortest. (b) Rural. (c) Mountainous. (d) Waterside. (e) Urban.

**Fig. 13** Five different routes provided to the participants between starting and destination points. These map images were captured from Google Maps.

(a) Rural 1. (b) Rural 2. (c) Rural 3. (d) Rural 4. (e) Rural 5.

**Fig. 14** Google Street View images for five waypoints on rural-prior routes. These street view images were captured from Google Street View.

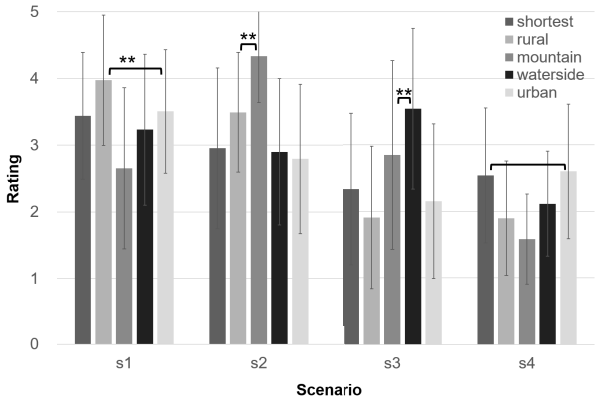


**Fig. 15** Results of the user evaluation. This figure shows the mean ratings of each route type for each scenario. The error bars show the standard deviation of each rating. A line with ** indicates that a significant difference ($p < 0.01/5$) could be confirmed between the first- and second-highest rated routes by a $z$-test (two-sided test). A line with no mark indicates that no significant difference could be confirmed.

nor unsuitable, unsuitable, strongly unsuitable).

In this evaluation, we used the same five pairs of starting and destination points as given in Section 5.4. For each pair, 30 participants evaluated routes on four scenarios. Consequently, 5 (pairs) × 30 (participants) = 150 ratings were obtained. Here, we allowed individual participants to evaluate multiple pairs.

After the evaluation, the participants voluntarily answered questions about their age, sex, and driving experiences for leisure purposes. For the driving experiences, the participants chose the best match among "*I often drive while enjoying landscapes*," "*I often drive while enjoying talking with passengers*," "*I often drive while enjoying driving itself*," "*I often drive while enjoying listening to music*," "*I rarely drive for leisure purposes*," "*I rarely drive at all*."

### 6.2 Participants

We recruited our participants through crowdsourcing. The number of participants was 58. The percentages of males and females were 70% and 30%, respectively. Participants who were 30–49 years old were 77% of the whole. Those under 30 years old represented 8%, and those over 49 years old represented 15%. For driving experiences, 47% chose "*I often drive while enjoying landscapes*." On the other hand, 19% chose either "*I rarely drive for leisure purposes*" or "*I rarely drive at all*."

### 6.3 Results

We treated the obtained Likert ratings as interval ratings and plotted them on a bar chart, as shown in **Fig. 15**.

For `s1`, `s2`, `s3`, and `s4`, the highest ratings were obtained for rural-, mountainous-, waterside-, and urban-prior routes, respectively. These results show that R3 can appropriately recommend roadscape-based routes without indicating which routes are which. For `s1`, `s2`, and `s3`, the results show significant differences ($p < 0.01/5$, with the Bonferroni correction applied); $p = 5.85 \times 10^{-6}$, 0.00, and $2.40 \times 10^{-7}$, respectively, by a paired $z$-test (two-sided). For `s4`, on the other hand, the results do not show significant differences; $p = 0.225$. As urban areas on Awaji Island (targeted in our experiment) are not very large, it was difficult for participants to recognize the urban-prior routes as routes that are truly urban. In the future, we would like to expand the scope of the areas.

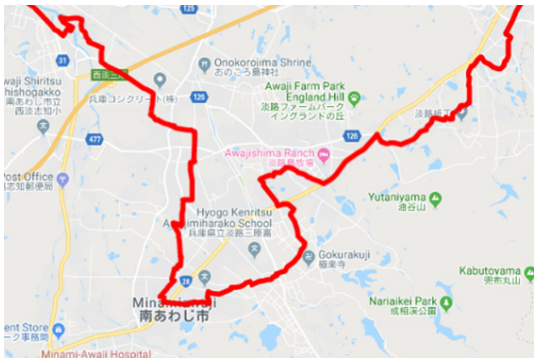


(a) Recommended route that includes many turning points. This map image was captured from Google Maps.

(b) Recommended route that includes narrow roads. This street view image was captured from Google Street View.

**Fig. 16** Limitations of the routes recommended by R3.

## 7. Limitations

In this paper, our focus with R3 is only on the roadscape features of road links. Therefore, considerations of the ease of driving, safety, and beauty of roadscapes is beyond the scope of this paper.

As two examples, **Fig. 16** shows parts of the routes recommended by R3. In the fine-grained route search, R3 focuses on the roadscape of a monolithic road link and does not consider the connections of adjacent links. Therefore, the recommended route shown in Fig. 16 (a) includes many turning points, which reduce the ease of driving. Figure 16 (b) shows a Street View im-

age of a particular point on the recommended mountainous-prior route. As shown in this figure, the road is very narrow, which reduces safety. In addition, our roadscape features do not necessarily reflect what people value. For example, although the view in Fig. 16 (b) is from the recommended mountainous-prior route, it is not always beautiful for people. One way of solving the above problems is to exploit external data such as social data, which include people's values.

## 8. Conclusions

In this paper, we have proposed R3, which provides diversified roadscape-based routes. Given starting and destination points, R3 provides four types of roadscape-based routes: rural-, mountainous-, waterside-, and urban-prior routes. To reduce computational costs, we proposed a coarse-to-fine route search approach that consists of a roadscape-based clustering method, roadscape cluster graph, coarse-grained route search, and fine-grained route search.

We evaluated the performance of R3 using real road network data with roadscape vectors, consisting of 102,506 road nodes and 212,050 road links in the area of Awaji Island. A comparison of the experimental results with Google satellite maps and Google Street View images qualitatively shows the validity of the generated roadscape clusters. The results also show the validity of the roadscape-based route recommendations. We qualitatively and quantitatively confirmed that R3 can provide routes reflecting each roadscape element. Furthermore, the results show that using a coarse-grained route search can significantly reduce the route search time. Finally, we quantitatively evaluated R3 from a user perspective. The results show that R3 can appropriately recommend roadscape-based routes for given scenarios.

Although we evaluated R3 using the road network data of Awaji Island, we will expand the scope of the areas, such as Kansai area in Japan. We would also like to consider the beauty of roadscapes by introducing some external data such as social data.

**Acknowledgments** This work was supported by JSPS KAKENHI, grant numbers JP15K12151 and JP16H05932.

### References

[1] Alivand, M. and Hochmair, H.: Extracting scenic routes from VGI data sources, *Proc. 2nd ACM SIGSPATIAL International Workshop on Crowdsourced and Volunteered Geographic Information*, pp.23–30 (2013).

[2] Alivand, M., Hochmair, H. and Srinivasan, S.: Analyzing how travelers choose scenic routes using route choice models, *Computers, Environment and Urban Systems*, Vol.50, pp.41–52 (2015).

[3] Arase, Y. and Xie, X.: Mining people's trips from large scale geotagged photos, *Proc. 18th ACM International Conference on Multimedia*, No.49, pp.133–142 (2010).

[4] Bellman, R.: ON A ROUTING PROBLEM, *Quarterly of Applied Mathematics*, Vol.16, No.1, pp.87–90 (1956).

[5] Byon, Y.-J., Abdulhai, B. and Shalaby, A.: Incorporating Scenic View, Slope, and Crime Rate into Route Choices: Emphasis on Three-Dimensional Geographic Information Systems with Digital Elevation Models and Crime Rate Geospatial Data, *Journal of the Transportation Research Board*, Vol.2183, No.1, pp.94–102 (2010).

[6] Chang, K.-P., Wei, L.-Y., Yeh, M.-Y. and Peng, W.-C.: Discovering personalized routes from trajectories, *Proc. 3rd ACM SIGSPATIAL International Workshop on Location-Based Social Networks*, Vol.1, pp.33–40, ACM Press (2011).

[7] Chen, Y.Y., Cheng, A.J. and Hsu, W.H.: Travel Recommendation by Mining People Attributes and Travel Group Types From Community-Contributed Photos, *IEEE Trans. Multimedia*, Vol.15, No.6, pp.1283–1295 (2013).

[8] Chen, Z., Shen, H.T. and Zhou, X.: Discovering Popular Routes from Trajectories, *Proc. 2011 IEEE 27th International Conference on Data*, Vol.4, pp.900–911 (2011).

[9] Chen, Z., Shen, H.T., Zhou, X., Zheng, Y. and Xie, X.: Searching trajectories by locations: An efficiency study, *Proc. 2010 ACM SIGMOD International Conference on Management of Data*, pp.255–266 (2010).

[10] Cheng, A.-J., Chen, Y.-Y., Huang, Y.-T., Hsu, W.H. and Liao, H.-Y.M.: Personalized travel recommendation by mining people attributes from community-contributed photos, *Proc. 19th ACM International Conference on Multimedia*, pp.83–92 (2011).

[11] Choudhury, M.D., Lempel, R., Israel, T. and Amer-yahia, S.: Automatic Construction of Travel Itineraries using Social Breadcrumbs, *Proc. 21st ACM Conference on Hypertext and Hypermedia*, pp.35–44 (2010).

[12] Chung, J. and Schmandt, C.: Going My Way: A User-aware Route Planner, *Proc. SIGCHI Conference on Human Factors in Computing Systems*, pp.1899–1902 (2009).

[13] Dechter, R. and Pearl, J.: Generalized best-first search strategies and the optimality af A*, *Journal of the ACM*, Vol.32, No.3, pp.505–536 (1985).

[14] Dijkstra, E.W.: A Note on Two Problems in Connexion with Graphs, *Numerische Mathematik*, Vol.1, pp.269–271 (1959).

[15] Goldberg, A.V. and Harrelson, C.: Computing the shortest path: A search meets graph theory, *Proc. 16th Annual ACM-SIAM Symposium on Discrete algorithms*, No.March 2003, pp.156–165 (2005).

[16] Gonzalez, H., Han, J. and Li, X.: Adaptive fastest path computation on a road network: A traffic mining approach, *Proc. 33rd International Conference on Very Large Data Bases*, pp.794–805 (2007).

[17] Herzog, D., Massoud, H. and Wörndl, W.: RouteMe: A Mobile Recommender System for Personalized, Multi-Modal Route Planning, *Proc. 25th Conference on User Modeling, Adaptation and Personalization*, pp.67–75 (2017).

[18] Hochmair, H.H. and Navratil, G.: Computation of scenic routes in street networks, *Proc. Geoinformatics Forum*, pp.124–133 (2008).

[19] Kanoulas, E., Du, Y., Xia, T. and Zhang, D.: Finding fastest paths on a road network with speed patterns, *Proc. 22nd International Conference on Data Engineering*, Vol.2006, p.10 (2006).

[20] Kurashima, T., Iwata, T., Irie, G. and Fujimura, K.: Travel route recommendation using geotags in photo sharing sites, *Proc. 19th ACM International Conference on Information and Knowledge Management*, pp.579–588, ACM Press (2010).

[21] Lu, X., Wang, C., Yang, J.-M., Pang, Y. and Zhang, L.: Photo2Trip: Generating travel routes from geo-tagged photos for trip planning, *Proc. 18th ACM International Conference on Multimedia*, pp.143–152 (2010).

[22] Luo, W., Tan, H., Chen, L. and Ni, L.M.: Finding time period-based most frequent path in big trajectory data, *Proc. 2013 ACM SIGMOD International Conference on Management of Data*, pp.713–724 (2013).

[23] Manzaki, S., Kano, A., Haneda, N., Sato, C. and Okude, N.: Country Road Finder: Exploring Beauty when Driving Around, *Proc. 2018 ACM Conference Companion Publication on Designing Interactive Systems*, pp.21–25 (2018).

[24] Niaraki, A.S. and Kim, K.: Ontology based personalized route planning system using a multi-criteria decision making approach, *Expert Systems with Applications*, Vol.36, No.2, pp.2250–2259 (2009).

[25] Oku, K. and Yamanishi, R.: Roadscape vectorization of road links based on extraction of raodscape elements from land cover map (in Japanese), *IPSJ SIG Technical Report*, Vol.2017-DBS-1, No.6, pp.1–6 (2017).

[26] Oku, K., Yamanishi, R., Matsumura, K. and Kawagoe, K.: Drive scenery estimation using image features extracted from roadmap and satellite images, *ISIS2015: Proc. 16th International Symposium on Advanced Intelligent Systems*, pp.1575–1589 (2015).

[27] Patel, K., Chen, M.Y., Smith, I. and Landay, J.A.: Personalizing Routes, *UIST 2006: Proc. 19th Annual ACM Symposium on User Interface Software and Technology*, pp.187–190 (2006).

[28] Potamias, M., Bonchi, F., Castillo, C. and Gionis, A.: Fast shortest path distance estimation in large networks, *Proc. 18th ACM Conference on Information and Knowledge Management*, pp.867–876 (2009).

[29] Quercia, D. and Aiello, L.M.: The Shortest Path to Happiness: Recommending Beautiful, Quiet, and Happy Routes in the City Categories and Subject Descriptors, *Proc. 25th ACM Conference on Hypertext and Social Media*, pp.116–125 (2014).

[30] Vieira, M.V., Fonseca, B.M., Damazio, R., Golgher, P.B., Reis, D.D.C. and Ribeiro-Neto, B.: Efficient search ranking in social networks, *Proc. 16th ACM Conference on Conference on Information and Knowledge Management*, pp.563–572 (2007).

[31] Wei, L.-Y., Peng, W.-C., Chen, B.-C. and Lin, T.-W.: Eleventh International Conference on Mobile Data Management PATS: A Framework of Pattern-Aware Trajectory Search, *Mobile Data Management*, pp.362–377 (2010).
[32] Wei, L.-Y., Peng, W.-C., Lin, C.-S. and Jung, C.-H.: Exploring Spatio-Temporal Features, *Advances in Spatial and Temporal Databases, Lecture Notes in Computer Science*, pp.399–404 (2009).
[33] Wei, L.-Y., Zheng, Y. and Peng, W.-C.: Constructing popular routes from uncertain trajectories, *Proc. 18th ACM SIGKDD International Conference on Knowledge Discovery and Data Mining*, pp.195–203 (2012).
[34] Yin, Z., Cao, L., Han, J., Luo, J. and Huang, T.: Diversified Trajectory Pattern Ranking in Geo-Tagged Social Media, *Proc. 2011 SIAM International Conference on Data Mining*, pp.980–991 (2011).
[35] Yoon, H., Zheng, Y., Xie, X. and Woo, W.: Smart Itinerary Recommendation Based on User-Generated GPS Trajectories, *International Conference on Ubiquitous Intelligence and Computing*, LNCS, Vol.6406, pp.19–34 (2010).
[36] Yoon, H., Zheng, Y., Xie, X. and Woo, W.: Social itinerary recommendation from user-generated digital trails, *Personal and Ubiquitous Computing*, Vol.16, No.5, pp.469–484 (2012).
[37] Yuan, J., Zheng, Y., Zhang, C. and Xie, W.: T-drive: Driving directions based on taxi trajectories, *Proc. 18th SIGSPATIAL International Conference on Advances in Geographic Information Systems*, pp.99–108 (2010).
[38] Yuan, J., Zheng, Y., Zhang, L., Xie, X. and Sun, G.: Where to find my next passenger, *Proc. 13th International Conference on Ubiquitous Computing*, pp.109–118 (2011).
[39] Zhang, J., Kawasaki, H. and Kawai, Y.: A tourist route search system based on Web information and the visibility of scenic sights, *Proc. 2nd International Symposium on Universal Communication*, pp.154–161 (2008).
[40] Zheng, Y.-T., Yan, S., Zha, Z.-J., Li, Y., Zhou, X., Chua, T.-S. and Jain, R.: GPSView: A scenic driving route planner, *ACM Trans. Multimedia Computing, Communications, and Applications*, Vol.9, No.1, pp.3:1–3:18 (2013).

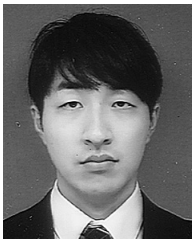

**Koji Kawamata** received his B.S. in Engineering, Department of Media Informatics, Faculty of Science and Technology, Ryukoku University, Japan in 2018. He is currently a M.S. student at Department of Media Informatics, Graduate School of Science and Technology, Ryukoku University, Japan.

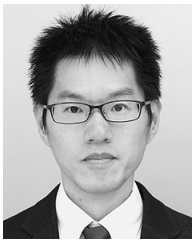

**Kenta Oku** received his B.S. in Engineering, Department of Civil Engineering, Osaka City University, Japan in 2004, M.S. in Engineering, Graduate School of Information Science, Nara Institute of Science and Technology, Japan in 2006, and Ph.D. in Engineering, Graduate School of Information Science, Nara Institute of Science and Technology, Japan in 2009. He is currently an Associate Professor, Faculty of Science and Technology, Ryukoku University, Japan. He was an Assistant Professor, College of Information Science and Engineering, Ritsumeikan University, Japan. His research interests are in the area of recommender systems.

(Editor in Charge: *Kaoru Hiramatsu*)